Published in final edited form as:
Gastroenterology. 2008 February ; 134(2): 511–522. doi:10.1053/j.gastro.2007.11.058.

A molecular signature of gastric metaplasia arising in response to acute parietal cell loss

Koji Nozaki[1,2], **Masako Ogawa**[2], **Janice A. Williams**[1], **Bonnie J. Lafleur**[1], **Vivian Ng**[3], **Ronny I. Drapkin**[3,4], **Jason C. Mills**[5], **Stephen F. Konieczny**[6], **Sachiyo Nomura**[2], and **James R. Goldenring**[1]

[1]Nashville VA Medical Center and the Department of Surgery, Vanderbilt-Ingram Cancer Center, Vanderbilt University School of Medicine, Nashville, Tennessee

[2]Department of Gastrointestinal Surgery, University of Tokyo, Tokyo, Japan

[3]Harvard Medical School, Dana-Farber Cancer Institute, Harvard Medical School, Boston, Massachusetts

[4]Department of Pathology, Brigham and Women's Hospital, Harvard Medical School, Boston, MA

[5]Department of Pathology and Immunology, Washington University School of Medicine, St Louis, Missouri

[6]Department of Biological Sciences and the Purdue Cancer Center, Purdue University, West Lafayette, Indiana

Abstract

Background & Aims—Loss of gastric parietal cells is a critical precursor to gastric metaplasia and neoplasia. However, the origin of metaplasia remains obscure. Acute parietal cell loss in gastrin-deficient mice treated with DMP-777 leads to the rapid emergence of Spasmolytic polypeptide/TFF2-expressing metaplasia (SPEM) from the bases of fundic glands. We have now sought to characterize more definitively the pathway for emergence of SPEM.

Methods—Emerging SPEM lineages in gastrin deficient mice treated with DMP-777 were examined for immunolocalization of TFF2, intrinsic factor and Mist1 and with electron microscopy. Emerging SPEM was isolated with laser capture microdissection and RNA was analyzed using gene microarrays. Immunohistochemistry in mouse and human samples was used to confirm up-regulated transcripts.

Results—DMP-777-induced SPEM was immunoreactive for TFF2 and the differentiated chief cell markers, Mist1 and intrinsic factor, suggesting that SPEM derived from transdifferentiation of chief cells. Microarray analysis of microdissected SPEM lineages induced by DMP-777 showed up-regulation of transcripts associated with G1/S cell cycle transition including MCM proteins, as well as a number of secreted factors, including HE4. HE4, which was absent in the normal

Address Correspondence: James R. Goldenring, M.D. Ph.D, Vanderbilt University School of Medicine, Department of Surgery, Epithelial Biology Program, 4160A MRBIII, 465 21st Avenue South, Nashville, TN 37232-2733, USA, TEL: (615) 936-3726, FAX: (615) 343-1591, jim.goldenring@vanderbilt.edu.

Conflict of interest: The authors have declared that no conflicts of interest exist.

stomach, was expressed in SPEM of human and mouse and in intestinal metaplasia and gastric cancer in humans.

Conclusion—While traditionally metaplasia was thought to originate from normal mucosal progenitor cells, these studies indicate that SPEM evolves through either transdifferentiation of chief cells or activation of a basal cryptic progenitor. Additionally, induction of metaplasia elicits the expression of secreted factors, such as HE-4, relevant to gastric pre-neoplasia.

Introduction

Gastric cancer remains the second leading cause of cancer-related death worldwide[1]. While the discrete mechanisms of gastric carcinogenesis remain obscure, one constant in the etiology of gastric cancer is the loss of acid secreting parietal cells from the fundic mucosa or oxyntic atrophy. The loss of parietal cells leads to alterations in the cells in the gastric mucosa with the emergence of metaplastic mucous cell lineages. The development of oxyntic atrophy and gastric cancer in humans is strongly linked through a sequence of lineage changes from normal to metaplastic to neoplastic[2]. Although *Helicobacter pylori* (*H. pylori*) infection is associated with the induction of atrophic gastritis and histological progression to gastric cancer, the exact mechanisms for the development of gastric metaplasia remain obscure. In addition to their important role in luminal HCl secretion, gastric parietal cells also secrete a number of critical paracrine and autocrine regulators including sonic hedgehog3 and the EGF receptor ligands TGFα, amphiregulin and HB-EGF[4]. Thus, loss of parietal cells may alter the intramucosal milieu leading to the initiation of metaplasia. It is now clear that two types of mucous cell metaplasia develop in the atrophic human stomach and represent putative pre-neoplastic lesions: goblet cell intestinal metaplasia and spasmolytic polypeptide-expressing metaplasia (SPEM, also known as pseudopyloric metaplasia)[5].

In the normal gastric fundic mucosa, progenitor cells located in the gland neck give rise to four types of epithelial cells including pepsinogen-secreting zymogenic chief cells, acid-producing parietal cells and two types of mucous cells: surface mucous cells and mucous neck cells[6]. Surface mucous cells secrete trefoil factor family 1 (TFF1) and mucin (MUC) 5 types A and C, whereas mucous neck cells secrete spasmolytic polypeptide/trefoil factor 2 (SP/TFF2) and MUC6. As mucous neck cells migrate towards the bases of fundic glands they re-differentiate into zymogenic chief cells, which secrete both pepsinogen and intrinsic factor in rodents[6]. The pre-zymogenic cells display granules showing features intermediate between those of neck cells and zymogenic chief cells. Importantly, the transition between mucous neck cells and chief cells occurs without an intermediate transiently amplifying cell and involves the induction of the transcription factor Mist1, a specific marker for mature chief cells7.

Several mouse models have sought to examine influences that may lead to metaplasia. Chronic infection with *Helicobacter felis* leads to oxyntic atrophy and the emergence of SPEM with the eventual development of dysplasia[8, 9]. Oral administration of DMP-777, a cell permeant inhibitor of neutrophil elastase, which also acts as a parietal cell specific protonophore[10], leads to the emergence of SPEM, but in the absence of a significant inflammatory response[11, 12]. While SPEM develops in wild type mice after 7–10 days of DMP-777 induced parietal cell loss, SPEM develops after only a single dose in gastrin-deficient mice[11]. Importantly, emerging SPEM cells express both TFF2 and the mouse chief cell marker intrinsic factor[11]. Thus, while prevailing dogma has suggested that metaplasias arise from aberrant differentiation of normal progenitor cells, these findings suggested that metaplastic SPEM cells were derived either from a cryptic progenitor cell population at the

bases of fundic glands or from transdifferentiation of chief cells expressing intrinsic factor into mucous cells expressing TFF2.

We now report that, in response to parietal cell loss, SPEM arises at the bases of gastric glands distinct from the normal progenitor cells. Loss of parietal cells leads to the observation of metaplastic cells expressing TFF2 along with the mature chief cell markers, intrinsic factor and Mist1. Microdissected emerging SPEM shows up-regulation of transcripts associated with G1/S cell cycle transition. In addition, transcripts for a group of secreted ligands were prominently up-regulated in SPEM. In particular, the WAP domain protein HE4 was absent from the normal stomach, but was strongly expressed in SPEM from mice, as well as in both SPEM and intestinal metaplasia in humans. HE4 was expressed in the vast majority of intestinal type and signet ring gastric adenocarcinomas. Our results indicate that SPEM likely develops initially from either transdifferentiation of chief cells or activation of a basal cryptic progenitor lineage. Furthermore, this metaplastic transition is associated with the upregulation of novel secreted mediators, such as HE-4, that could serve as surrogate markers of the pre-neoplastic process.

Materials and Methods

Gene Microarray Analysis

Gastrin-deficient mice were constructed by targeted disruption of the gastrin gene and were maintained on a C57BL/6 background[11]. Mice were treated for 1 or 3 days with oral gavage administration of DMP-777 (a gift of DuPont Pharmaceuticals), formulated in 0.5% methylcellulose (administered orally as a gavage once daily at 350 mg/kg/day). Untreated mice were utilized as controls. Mice were sacrificed and their stomachs were excised and opened along the greater curvature and processed for frozen sections for laser capture microdissection. From the untreated Gastrin-deficient mice, chief cells were microdissected from the bases of gastric glands. The emerging SPEM cells were microdissected from the bases of fundic glands of DMP-777-treated Gastrin-deficient mice after 1 or 3 days of oral drug administration. Cell collections (10,000 cells) and extractions of total RNA were performed as previously described[12].

Total RNAs from microdissected cells were reverse transcribed and amplified through two rounds of linear amplification using a Nugen Ovation kit to amplify and label 10–20 ng of RNA. The resulting single-strand cDNA product was purified by binding to and elution from a Qiagen Qiaquick column. The cDNA product was then quantitated and 2.2 μg of the fragmented, labeled product was hybridized to Affymetrix Mouse 430 2.0 microarrays overnight, with staining and scanning performed the next day (Vanderbilt Microarray Facility). Gene expression was analyzed among microdissected cells from 4 untreated gastrin deficient mice, 4 mice treated with DMP-777 for one day and 4 mice treated with DMP-777 for three days. The raw gene expression data (.cel files) were converted to expression values using the Affy function in R (http://www.bioconductor.org). The expression levels between groups were compared first using an overall permutation F-test for difference between the groups (control, one day treatment and three days of treatment) using analysis of variance; if a statistically significant overall difference was seen then pair-wise differences between control and one day of treatment and control and three days of treatment were performed using permutation t-tests. We then further reduced the candidate probe list by requiring at least 2-fold differences between treated groups (day 1 and day 3) and control in those that showed a statistically significant pair-wise difference. All expression data analysis was performed using the SAFE package in R. Annotation and pathways were interrogated using the WebGestalt software[13].

Quantitative Polymerase Chain Reaction

Independent of the samples collected from animals for microarray analysis, total RNA isolated from laser-capture microdissected cell collections from the stomachs of normal and DMP-777 1-day-treated and DMP-777 3-day–treated gastrin-deficient mice was analyzed by quantitative PCR assays. Reverse transcription from each total RNA sample was performed using random primers and Quantiscript Reverse transcriptase (Qiagen), for 30 minutes at 42°C. Quantitative real-time PCR was performed with a 3-step method using the Bio-Rad iCycler iQ real-time PCR detection system (Bio-Rad Laboratories, Hercules, CA). Each reaction was carried out in a 50 μL mixture consisting of QuantiTect SYBR Green PCR Master Mix (Qiagen), and 1 μL of template cDNA. The sequences of the primers used are listed in Supplementary Table 1. The PCR conditions for quantitative real-time PCR were: 95°C for 10 minutes, 45 cycles of 94°C for 15 seconds, 60°C for 30 seconds, and 72°C for 30 seconds. Quantitation of cDNA template in each sample was determined using the comparative threshold cycle (C_T) method using GAPDH as a control, as described previously[12]. Statistical comparisons of the mean $\Delta\Delta C_T$ between groups were determined using the Mann-Whitney *U* Test.

Immunohistochemistry

Excised stomachs from Gastrin-deficient mice treated with DMP-777 or untreated controls embedded in paraffin were used for immunohistochemistry analysis. Stomachs from C57BL/6 wild–type mice and sections from *H. felis*-infected C57BL/6 mice (infected for 6 month, a gift from Dr. Timothy C. Wang, Columbia University, New York, NY) were also examined with staining as a comparison. For immunohistochemistry, except for Mist1 staining, deparaffinized sections were pretreated with antigen retrieval using Target Retrieval solution (DakoCytomation) at 120°C for 15 minutes, followed by immediate cooling using iced water. For immunohistochemistry of Mist1, Trilogy antigen retrieval solution (Cell Marque, Austin, TX) was used during the antigen retrieval procedure. Sections were treated with 2% blocking serum and then incubated with the primary antibody overnight at 4°C. Immunostaining was performed with the following primary antibodies: murine monoclonal immunoglobulin M (IgM) anti-trefoil factor family 2 (TFF2, a gift from Sir Nicholas Wright, Cancer Research UK; 1:1000); rabbit anti-Mist1 (1:2000)7; murine monoclonal anti-H/K-ATPase (a gift from Dr. Adam J. Smolka, Medical University of South Carolina; 1:100,000); rabbit anti-HE4 (1:2000)14; rabbit anti-Intrinsic factor (a gift from Dr. David Alpers, Washington University, St. Louis; 1:2000); goat anti-Intrinsic factor (1:2000)7; rabbit anti-MCM3 (a gift from Dr. Jin Woo Kim, Catholic University of Korea; 1:2000); rat monoclonal anti-Ki67 (TEC-3, DakoCytomation; 1:200).

For immunofluorescence analysis, Cy3-goat anti-mouse IgM antibody, Cy5-goat anti-mouse IgG antibody (Jackson ImmunoResearch) and Alexa488 goat anti-rabbit IgG (Invitrogen) were used. ProLong Gold Antifade Reagent with DAPI (Invitrogen) was used for nuclear counterstain and mounting medium.

For immunohistochemistry with detection with diaminobenzidine, the sections were incubated with biotinylated secondary antibody followed by horseradish peroxidase-conjugated streptavidin. Chromogen was developed with diaminobenzidine (Biogenex). For immunohistochemistry with alkaline-phosphatase detection, the sections were incubated with biotinylated secondary antibody followed by alkaline phosphatase-conjugated avidin-biotin complex. Chromogen was developed with Vector Red Substrate (Vector Laboratories). All sections were counterstained with Gill's hematoxylin.

Sections were viewed and photographed on Zeiss Axiophot microscope equipped with an Axiovision digital imaging system (Zeiss) or FluoView FV1000 confocal microscope system (Olympus).

Two tissue arrays were utilized for staining of human stomach samples as previously described[15]. One tissue array contained samples of normal gastric mucosa and examples of SPEM and intestinal metaplasia from 33 gastric resections at the University of Tokyo. The second array contained normal mucosa and gastric adenocarcinomas from 44 patients resected at Vanderbilt.

Electron microscopy analysis

Fresh specimens from the gastric fundic region of untreated controls and 3-day DMP-777 treated gastrin-deficient mice were fixed for 2.5 hour on ice in 2.5% glutaraldehyde, 0.1M cacodylate buffer in PBS. The samples were incubated overnight at 4°C in 1% osmium tetroxide (OsO_4) and 0.1M Cacodylate Buffer. Subsequently, the samples were subjected to an ethanol dehydration series and embedded in Spurrs resin. 50–100 nm thin sections were cut and collected on 200-mesh, formvar-coated copper grids. After drying overnight, the grids were contrast stained with 2% depleted Uranyl Acetate (UA) and then stained with saturated lead citrate. Samples were examined on a Philips CM12 Electron Microscope.

Results

Morphological evidence for transdifferentiation

Given previous results suggesting the rapid evolution of SPEM in gastrin-deficient mice[11], we evaluated whether mature chief cells expressing the bHLH transcription factor Mist1 could give rise to SPEM in DMP-777-treated mice[7]. In untreated gastrin-deficient mice, the nuclei of mature chief cells stained with antibodies against Mist1, and mucous neck cells stained with TFF2 antibodies (Figure 1A). In contrast, in mice treated with DMP-777 for three days, the number of Mist1 immunoreactive cells decreased at the bases of glands, and a number of the Mist1 positive cells were dual immunoreactive for TFF2 (Figure 1, B–C). In the normal stomach, TFF2 and intrinsic factor were expressed in secretory granules of either mucous neck cells or chief cells, respectively (Figure 1D). However, in gastrin deficient mice treated for 3 days with DMP-777, SPEM cells expressing two separate populations of TFF2 and intrinsic factor staining granules were present at the bases of fundic glands (Figure 1, E–F). These results suggested that the loss of parietal cells in DMP-777-treated mice induced a marked alteration in the cellular phenotype of chief cells.

To examine cell lineages more precisely, the chief cells from untreated gastrin-deficient mice and emerging SPEM cells from gastrin-deficient mice treated for 3 days with DMP-777 were examined by electron microscopy (Figure 1, G–I). In untreated animals, normal chief cells were observed with uniformly staining zymogen granules (Figure 1G). However, in the DMP-777-treated cells, a heterogeneous set of granule morphologies was observed in SPEM cells at the bases of fundic glands (Figure 1, H–I). The SPEM cells did contain some normal appearing zymogen granules, generally in the perinuclear region, but they also showed large granules with electron dense material and single electron lucent circular peripheral inclusions, a morphology more consistent with mucous secretory granules. In addition, numerous smaller electron lucent granules were observed in the sub-luminal region. These changes in chief cell granule morphologies were observed with no morphological evidence of apoptosis. These results indicated that chief cells were altering their granule contents to adopt morphologies more similar to mucous secreting cells[7].

Gene microarray analysis of the emergence of SPEM

To analyze alterations in gene expression attendant with the emergence of SPEM, we utilized laser capture microdissection to isolate chief cells from untreated gastrin-deficient mice as well as the emerging SPEM cells from mice treated with DMP-777 for either one or three days. Affymetrix gene microarrays were probed with the mRNAs prepared from microdissected cells. Table 1 demonstrates that DMP-777 treatment led to the rapid up-regulation of a number of transcripts after only one dose of drug. Pathway analysis showed that the most prominent sets of transcripts were involved in cell cycle regulation and nucleotide metabolism (Table 1A). In particular, 28 out of the top 50 probes for up-regulated transcripts detected messages for proteins implicated in the regulation of the G1/S transition including 5 MCM proteins, ATF3, Ris2, RAD51 and ligase1. No pro-apoptotic genes were detected in the cohort of up-regulated gene transcripts in both 1 and 3 days of DMP-777-treatment (Supplemental Table 2). No clear pattern of gene transcript down-regulation was observed (Supplemental Table 3), although it is notable that there was a significant decrease in transcripts for pancreatic lipase-related protein 1 (PNLIPRP1), a chief cell product. In addition to the up-regulation of G1/S modulators, we also observed the prominent up-regulation of the expression for a number of secreted regulators including two WAP domain proteins, WFDC2 (HE4) and WDNM1 (Expi), Interleukin-1 receptor antagonist (IL1RN) and Epiregulin (Table 1B).

Quantitative PCR analysis of the emergence of SPEM

To validate the results of the gene microarray studies, we evaluated the expression of selected up-regulated or down-regulated transcripts in microdissected lineages using quantitative PCR. We confirmed the up-regulation of G1/S associated transcripts including MCM3, MCM5, MCM7 and ATF3 (Figure 2). We also confirmed the up-regulation of transcripts for putative soluble mediators including HE4 and IL1RN and confirmed the down-regulation ST3Gal6. We have previously noted that Affymetrix gene arrays do not detect accurately changes in TFF2 expression[12]. However, by quantitative PCR assays, TFF2 levels were elevated greater than 7-fold in emerging SPEM from DMP-777 treated animals (Figure 2). Finally, to assess the loss of differentiated chief cell markers we also evaluated transcript levels for pancreatic lipase-related proteins 1 and 2, pepsinogens A and C and Mist1. Supplemental Figure 1A demonstrates that there was a significant decrease in mRNA transcripts for all four protein markers. In correlation, with these findings, we also observed a rapid loss of Mist1 immunostaining at the bases of fundic gastric glands that was sustained out to 7 days of DMP-777 treatment (Supplemental Figure 1B–D).

MCM3 and TACC3 expression is increased following acute oxyntic atrophy

To investigate the up-regulation of transcripts involved in G1/S transition, we examined the stomachs of DMP-777-treated or untreated gastrin-deficient mice with dual-staining with antibodies against MCM3 and Ki67, a general marker of proliferating cells (Figure 3). In untreated mice, MCM3 was predominantly localized to cells within the normal progenitor zone located in the neck region of the glands (Figure 3A). Nevertheless, occasionally we did observe nuclear MCM3 expression in cells at the bases of fundic glands (Figure 3A). In DMP-777 treated mice, in addition to MCM3 staining in the proliferative neck region, we also observed prominent nuclear staining in SPEM cells at the bases of the fundic glands (Figure 3, B–E). MCM3 expressing cells were more widely distributed within SPEM cells compared to Ki67 labeled cells. While Ki67 positive cell numbers showed only a small increase after DMP-777 treatment, the number of MCM3 positive cells increased after 1 day of DMP-777 (Figure 3B) treatment and remained elevated through 14 days of treatment (Figure 3, C–E). The findings with Ki67 were similar to those with BrdU labeling (data not shown). The results suggest that MCM3 activation in emerging SPEM is more prominent than active entry into the cell cycle (Figure 3F).

While these results indicated that SPEM cells emerging from the bases of gastric glands expressed MCM3, we also sought to understand the identity of MCM3 staining cells at the bases of glands in untreated mice. The observation was not specific to gastrin deficient mice, since similar MCM3-expressing cells were observed at the bases of glands in wild type C57BL/6 mice (data not shown). We therefore performed dual staining of sections for both MCM3 and intrinsic factor, a marker of mature chief cells (Figure 4). In all cases, cells with MCM3 staining nuclei at the bases of glands were also immunoreactive for intrinsic factor, indicative of chief cells (Figure 4F).

We also examined that expression of TACC3, a protein associated with the initiation of cell cycle[16], in DMP-777-treated mouse stomachs. While little TACC3 expression was noted in the stomachs of untreated mice (Supplemental Figure 2), TACC3 expression was strongly up-regulated in SPEM cells at the bases of fundic glands following treatment with DMP-777 for 3 days (Supplemental Figure 2).

Up-regulation of HE4 in gastric metaplasia and cancer

As noted above, emergence of SPEM also coincided with up-regulation of several secreted factors. We therefore performed immunostaining for the WAP domain protein HE4 in gastrin-deficient mice. Immunostaining showed little detectable HE4 in the normal gastric mucosa of gastrin-deficient (Figure 5A) or wild-type C57BL/6 mice (data not shown). Nevertheless, in DMP-777 treated mice, we observed a prominent up-regulation of HE4 expression in SPEM cells at the bases of fundic glands (Figure 5B). In immunofluorescence studies, HE4 granules stained distinctly from TFF2 staining granules in SPEM cells (data not shown). To evaluate whether HE4 up-regulation was a common characteristic of SPEM, we also evaluated HE4 staining in the mucosa of C57BL/6 mice infected with *Helicobacter felis* for 9 months. Prominent HE4 staining was observed in SPEM cells throughout the fundic mucosa in *Helicobacter felis*-infected mice (Figure 5C).

Since the studies in mice suggested a strong association of HE4 expression with gastric metaplasia, we evaluated the expression of HE4 in the human stomach. As noted previously[17], HE4 was not detected in the normal human fundic mucosa (Figure 5D). Notably, the tissue array analysis showed that HE4 was positive in all metaplastic lesions, including SPEM (Figure 5E), SPEM and intestinal metaplasia transitional lesions (Figure 5F), SPEM and intestinal metaplasia co-existing lesions (Figure 5G–H), and intestinal metaplasia (Figure 5I). Given the strong expression of HE4 in human gastric metaplasias, we also examined the expression of HE4 in human gastric adenocarcinoma. In contrast with TFF2, which shows a general loss in gastric cancer[14], we observed sustained expression of HE4 in 70% of well and moderately-differentiated intestinal type gastric adenocarcinomas (Figure 6A–D). 20% of diffuse or poorly differentiated tumors also showed HE4 staining (Figure 6E–F). The HE4 staining was especially strong in 80% of signet ring adenocarcinomas (Figure 6G–I). Similar results were observed with immunofluorescence staining, supporting the histochemical staining results for HE4 (Figure 6J–L). These results indicate that HE4 is a robust biomarker for the gastric pre-neoplasia and the neoplastic process.

Discussion

The loss of parietal cells, oxyntic atrophy, is the most reliable correlate with gastric cancer in humans. The results presented here suggest that the loss of parietal cells in gastrin-deficient mice leads to the rapid appearance of metaplastic cells at the bases of fundic glands expressing both mature chief cell markers and TFF2. Attendant with this process, we observed an up-regulation of genes involved in G1/S phase transition leading to re-entry of a population of cells into the cell cycle. The metaplastic process was also associated with the

up-regulation of a number of putative soluble regulators not usually present in the normal stomach mucosa. In particular, HE4 was up-regulated in gastric metaplasia in both mice and humans and its expression was maintained in gastric adenocarcinomas. Thus, examination of the induction of gastric metaplasia in mice has revealed a number of critical regulators relevant to the pre-neoplastic process in humans.

While most views of the stomach mucosa have centered on lineage production from the normal progenitor zone in the neck of gastric fundic glands[6], the present investigations focus attention on a potential compartment at the bases of fundic glands induced following parietal cell loss[11]. Three explanations could account for this observation (Figure 7). First, a cryptic progenitor cell population may exist at the base of fundic glands, distinct from the normal progenitor region in the neck, which would be suppressed by mucosal differentiation factors released by parietal cells. At least in gastrin-deficient mice, this explanation seems less likely because of the rapidity of metaplastic changes and the low amount of proliferation.

Second, SPEM may develop from transdifferentiation of chief cells (Figure 7). Previous studies have demonstrated that acute oxyntic atrophy leads to the observation of proliferating cells expressing intrinsic factor, a marker of differentiated chief cells in mice[11]. Whereas intrinsic factor is expressed in rare pre-zymogenic cells, Mist1 is expressed only in mature chief cells[7]. The observation here of Mist1-immunoreactive cells also expressing TFF2 supports chief cell transdifferentiation as the origin of SPEM. The transdifferentiation of zymogenic cells to mucous metaplasia may be a general mechanism underlying pre-neoplastic transition in the upper gastrointestinal tract. Means, et al. have demonstrated that over-expression of TGFα leads to the transdifferentiation of pancreatic zymogen cells into mucous secreting metaplastic cells[18]. Acinar cell transdifferentiation contributes to pre-neoplastic PANIN lesion formation in the pancreas[19]. Likewise, loss of parietal cells may elicit the transdifferentiation of gastric zymogen-secreting chief cells. Nevertheless, these findings may also support a model compatible with both foregoing hypotheses (Figure 7). MCM3, which is required for unwinding of DNA during the G1/S transition, was expressed not only in normal progenitor cells in the gastric gland neck, but also in a small population of intrinsic factor-immunoreactive chief cells at the bases of fundic glands. Thus, a sub-population of chief cells may have the potential for transdifferentiation, in effect a cryptic progenitor population. Still, the rapid emergence of SPEM at the base of gastric glands in the gastrin-deficient mice after DMP-777 treatment suggests that a broader transdifferentiative process is required to account for the amount of SPEM observed after only 1 or 3 days of treatment.

Finally, it is possible that the observed lineage changes could result from arrest of chief cell lineage differentiation from mucous neck cells (Figure 7). Again, the rapidity of changes and the morphological changes in chief cells at the bases of glands without evidence of apoptosis would seem to militate against this hypothesis. Nevertheless, it should be noted that over time with continued oxyntic atrophy, it is possible that the extent of SPEM observed may reflect in part an arrest of chief cell differentiation. We have suggested such a mechanism in studies of amphiregulin-deficient mice treated with DMP-777[20].

The gene microarray studies of microdissected SPEM cells also support a molecular phenotype for SPEM induction. We observed the rapid up-regulation after only a single dose of DMP-777 of a cohort of gene transcripts related to the initiation of the G1/S cell cycle transition. MCM proteins (MCM2-7) are transcribed at M/G1 and assemble into a DNA helicase responsible for unwinding chromatin prior to DNA synthesis[21]. MCM3 is ubiquitinated specifically in G2/M and degraded as cells exit mitosis. Still, while MCM proteins are broadly up-regulated in SPEM at the bases of fundic glands in DMP-777-treated mice, we have observed only a subset of cells entering the proliferative cycle. Thus,

although some cells are re-entering the cell cycle, the observation of the up-regulation of a number of proteins involved in G1/S transition is also consistent with an alternative hypothesis. Transdifferentiation would require a major alteration in the compendium of transcripts expressed in cells without necessarily going through a proliferative cycle. Such a change in transcripts would require the unwinding of DNA, just as at the G1/S cell cycle interface. Thus, the up-regulation of proteins involved in DNA remodeling may reflect more the process of transdifferentiation than activation of proliferation. The sustained expression of MCM3 in DMP-777 treated mice supports the concept of an alteration of the compendium of transcripts during transdifferentiation, with only limited progression through the cell cycle.

The findings presented here also suggest that acute oxyntic atrophy leads to up-regulation of gene transcripts specific for mucous cell metaplasia. The emergence of mucous cell metaplasia up-regulated specific secreted mucosal factors, including HE4, WDNM1, IL1RN and Epiregulin. IL1RN has been implicated in a number of neoplastic processes22. Similarly, Epiregulin, an EGF receptor ligand family member with affinity for Erb4, is associated with more aggressive cancer metastasis23. HE4 is up-regulated early in the development of ovarian cancer and may serve as a biomarker of ovarian neoplasia[14]. While HE4 is not expressed in the normal human gastric mucosa, we observed prominent up-regulation of HE4 expression in both intestinal metaplasia and SPEM. Importantly, HE4 expression was maintained in the vast majority of differentiated gastric adenocarcinomas. We have also observed increased expression of HE4 in PANIN lesions and pancreatic adenocarcinoma (unpublished data). The current study therefore shows that factors up-regulated in the process of SPEM induction also may serve as surrogate biomarkers of gastric pre-neoplasia and neoplasia.

In summary, while previous views have suggested that gastric metaplasia originates from normal mucosal progenitor cells, the present results indicate that the loss of parietal cells from the gastric fundic mucosa induces alterations in the transcriptional profile of chief cells leading to changes in the cellular secretory phenotype and transdifferentiation into a mucous cell metaplasia. Attendant with these changes, particular soluble regulators such as HE4 are up-regulated in metaplasia and represent characteristic putative biomarkers for the metaplastic and pre-neoplastic process.

Supplementary Material

Refer to Web version on PubMed Central for supplementary material.

Abbreviations

SPEM	spasmolytic polypeptide expressing metaplastic lineage
IM	Intestinal Metaplasia
TFF2	trefoil factor family 2
HE4	human epididymis 4
WFDC2	WAP 4-disulfide core domain 2
WAP	Whey Acidic Protein
MCM	minichromosome maintenance deficient
TACC3	transforming acidic coiled-coil containing protein 3

Acknowledgments

We thank Drs. Adam Smolka, Jin Woo Kim, Nicholas Wright and David Alpers for the gifts of antibodies. We thank Dr. Timothy Wang for continuing discussions and sections of stomach from *H. felis*-infected mice. We thank Dr. Joseph Roland for artistic contributions. These studies were supported by grants to J.R.G. from a Department of Veterans Affairs Merit Review Award, a pilot project grant from the Vanderbilt SPORE in Gastrointestinal Cancer (1P 50 CA95103), the AGA Funderburg Award in Gastric Biology Related to Cancer, and a Discovery Grant from the Vanderbilt-Ingram Cancer Center. J.C.M. was supported by NIH K08 DK066062 and S.F.K. was supported by NIH RO1 DK55489. R.D. was supported by NIH K08 CA108748, the Ovarian Cancer Research Fund (OCRF), the Fannie E. Rippel Foundation, and the Dunkin Donuts Rising Stars Program. K.N. was supported by the Jon Isenberg Award from the Foundation for Digestive Health and Nutrition /American Gastroenterological Association (FDHN/AGA).

References

1. Pisani P, Bray F, Parkin DM. Estimates of the world-wide prevalence of cancer for 25 sites in the adult population. Int J Cancer 2002;97:72–81. [PubMed: 11774246]
2. Parsonnet J, Friedman GD, Vandersteen DP, Chang Y, Vogelman JH, Orentreich N, Sibley RK. Helicobacter pylori infection and the risk of gastric cancer. New Eng.J.Med 1991;325:1127–1131. [PubMed: 1891020]
3. Stepan V, Ramamoorthy S, Nitsche H, Zavros Y, Merchant JL, Todisco A. Regulation and function of the sonic hedgehog signal transduction pathway in isolated gastric parietal cells. J Biol Chem 2005;280:15700–15708. [PubMed: 15691835]
4. Beauchamp RD, Barnard JA, McCutchen CM, Cherner JA, Coffey RJ Jr. Localization of transforming growth factor alpha and its receptor in gastric mucosal cells. J.Clin.Invest 1989;84:1017–1023. [PubMed: 2760208]
5. Schmidt PH, Lee JR, Joshi V, Playford RJ, Poulsom R, Wright NA, Goldenring JR. Identification of a metaplastic cell lineage associated with human gastric adenocarcinoma. Lab.Invest 1999;79:639–646. [PubMed: 10378506]
6. Karam SM, Leblond CP. Dynamics of epithelial cells in the corpus of the mouse stomach. III. Inward migration of neck cells followed by progressive transformation into zymogenic cells. Anat.Rec 1993;236:297–313. [PubMed: 8338234]
7. Ramsey VG, Doherty JM, Chen CC, Stappenbeck TS, Konieczny SF, Mills JC. The maturation of mucus-secreting gastric epithelial progenitors into digestive-enzyme secreting zymogenic cells requires Mist1. Development 2007;134:211–222. [PubMed: 17164426]
8. Houghton J, Stoicov C, Nomura S, Carlson J, Li H, Rogers AB, Fox JG, Goldenring JR, Wang TC. Gastric cancer originating from bone marrow derived cells. Science 2004;306:1568–1571. [PubMed: 15567866]
9. Wang TC, Dangler CA, Chen D, Goldenring JR, Koh T, Raychowdhury R, Coffey RJ, Ito S, Varro A, Dockray GJ, Fox JG. Synergistic interaction between hypergastrinemia and Helicobacter infection in a mouse model of gastric cancer. Gastroenterology 2000;118:36–47. [PubMed: 10611152]
10. Goldenring JR, Ray GS, Coffey RJ, Meunier PC, Haley PJ, Barnes TB, Car BD. Reversible drug-induced oxyntic atrophy in rats. Gastroenterology 2000;118:1080–1093. [PubMed: 10833483]
11. Nomura S, Yamaguchi H, Wang TC, Lee JR, Goldenring JR. Alterations in gastric mucosal lineages induced by acute oxyntic atrophy in wild type and gastrin deficient mice. Amer.J.Physiol 2004;288:G362–G375.
12. Nomura S, Baxter S, Yamaguchi T, Leys C, Vartapetian AB, Fox JG, Lee JR, Wang TC, Goldenring JR. Spasmolytic polypeptide expressing metaplasia (SPEM) to pre-neoplasia in *H. felis*-infected mice. Gastroenterology 2004;127:582–594. [PubMed: 15300590]
13. Zhang B, Kirov S, Snoddy J. WebGestalt: an integrated system for exploring gene sets in various biological contexts. Nucleic Acids Res 2005;33:W741–W748. [PubMed: 15980575]
14. Drapkin R, von Horsten HH, Lin Y, Mok SC, Crum CP, Welch WR, Hecht JL. Human epididymis protein 4 (HE4) is a secreted glycoprotein that is overexpressed by serous and endometrioid ovarian carcinomas. Cancer Res 2005;65:2162–2169. [PubMed: 15781627]

15. Leys CM, Nomura S, Rudzinski E, Kaminishi M, Montgomery E, Washington MK, Goldenring JR. Expression of Pdx-1 in human gastric metaplasia and gastric adenocarcinoma. Hum Pathol 2006;37:1162–1168. [PubMed: 16938521]

16. Aitola M, Sadek CM, Gustafsson JA, Pelto-Huikko M. Aint/Tacc3 is highly expressed in proliferating mouse tissues during development, spermatogenesis, and oogenesis. J Histochem Cytochem 2003;51:455–469. [PubMed: 12642624]

17. Bingle L, Singleton V, Bingle CD. The putative ovarian tumour marker gene HE4 (WFDC2), is expressed in normal tissues and undergoes complex alternative splicing to yield multiple protein isoforms. Oncogene 2002;21:2768–2773. [PubMed: 11965550]

18. Means AL, Meszoely IM, Suzuki K, Miyamoto Y, Rustgi AK, Coffey RJ Jr, Wright CV, Stoffers DA, Leach SD. Pancreatic epithelial plasticity mediated by acinar cell transdifferentiation and generation of nestin-positive intermediates. Development 2005;132:3767–3776. [PubMed: 16020518]

19. Zhu L, Shi G, Schmidt CM, Hruban RH, Konieczny SF. Acinar cells contribute to the molecular heterogeneity of pancreatic intraepithelial neoplasia. Am J Pathol 2007;171:263–273. [PubMed: 17591971]

20. Nam KT, Varro A, Coffey RJ, Goldenring JR. Potentiation of oxyntic atrophy-induced gastric metaplasia in amphiregulin-deficient mice. Gastroenterology 2007;132:1804–1819. [PubMed: 17484876]

21. Braun KA, Breeden LL. Nascent transcription of MCM2-7 is important for nuclear localization of the minichromosome maintenance complex in G1. Mol Biol Cell 2007;18:1447–1456. [PubMed: 17314407]

22. Machado JC, Pharoah P, Sousa S, Carvalho R, Oliveira C, Figueiredo C, Amorim A, Seruca R, Caldas C, Carneiro F, Sobrinho-Simoes M. Interleukin 1B and interleukin 1RN polymorphisms are associated with increased risk of gastric carcinoma. Gastroenterology 2001;121:823–829. [PubMed: 11606496]

23. Gupta GP, Nguyen DX, Chiang AC, Bos PD, Kim JY, Nadal C, Gomis RR, Manova-Todorova K, Massague J. Mediators of vascular remodelling co-opted for sequential steps in lung metastasis. Nature 2007;446:765–770. [PubMed: 17429393]

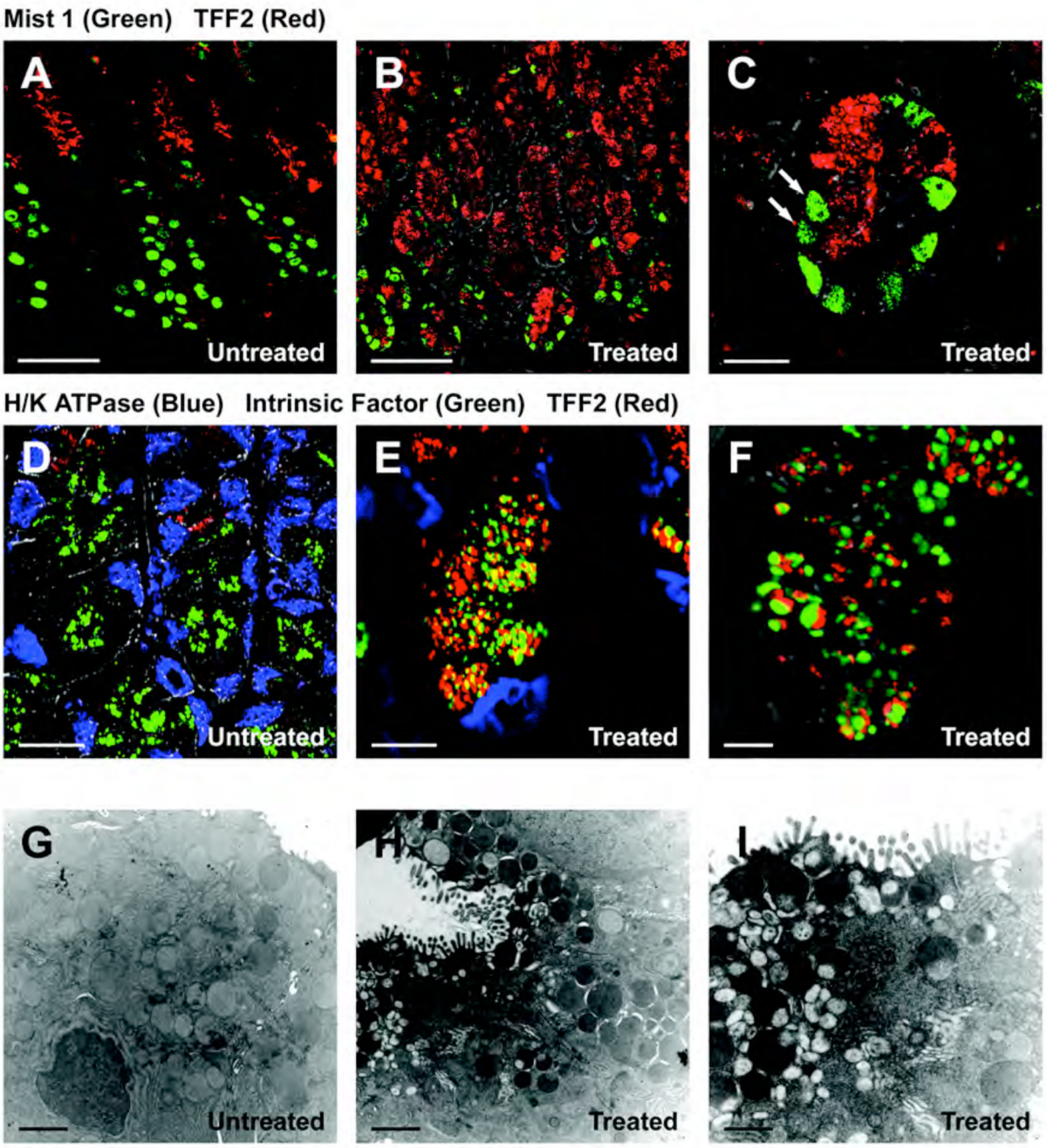

Figure 1. Characterization of emerging SPEM

(A) Fundic mucosa from an untreated gastrin deficient mouse was dual immunostained for Mist1 (green) and TFF2 (red). Mist1 antibodies stained the nuclei of mature chief cells at the base of fundic glands, while TFF2 was positive in mucous neck cells in the neck region of the fundic gland. No discernible dual staining cells were observed (Scale bar: 50 μm). **(B, C)** Mist1 and TFF2 expression in a gastrin-deficient mouse treated with DMP-777 for 3 days. The number of Mist1 immunoreactive cells (green) decreased in the bottom of glands, and a number of the Mist1 positive cells were dual immunoreactive for TFF2 (red). (Scale bar: **B**, 50 μm; **C**, 10 μm) The high power view in **C**. demonstrates the presence of cells dual labeled for Mist1 and TFF2 (arrows). **(D)** Mucosa from an untreated mouse stained with

antibodies for the H/K-ATPase (blue), TFF2 (red) and Intrinsic factor (green). Note that there was no overlap in the staining of the three lineages (Scale bar: 20 μm). **(E, F)** Mucosa from a mouse treated with DMP-777 for 3 days stained with antibodies for the H/K ATPase (blue), TFF2 (red) and Intrinsic factor (green). While parietal cells only stained with H/K-ATPase antibodies, SPEM cells at the base of the glands stained for both intrinsic factor (green) and TFF2 (red). The higher power view in **F**. demonstrates the presence of two separate populations of vesicles in the SPEM cells. (Scale bar: **E**, 10 μm; **F**, 4 μm). **(G, H, I)** Electron micrographs of chief cells from an untreated mouse **(G)** and emerging SPEM cells from a 3 day DMP-777-treated mouse **(H, I). (G)** Chief cells showed uniformly staining zymogen granules (Scale bar: 2 μm). **(H, I)** SPEM cells at the base of fundic glands of a mouse treated with DMP-777 for 3 days contained a heterogeneous set of granule morphologies. (Scale bar: **G, H**, 2 μm; **I**, 1 μm).

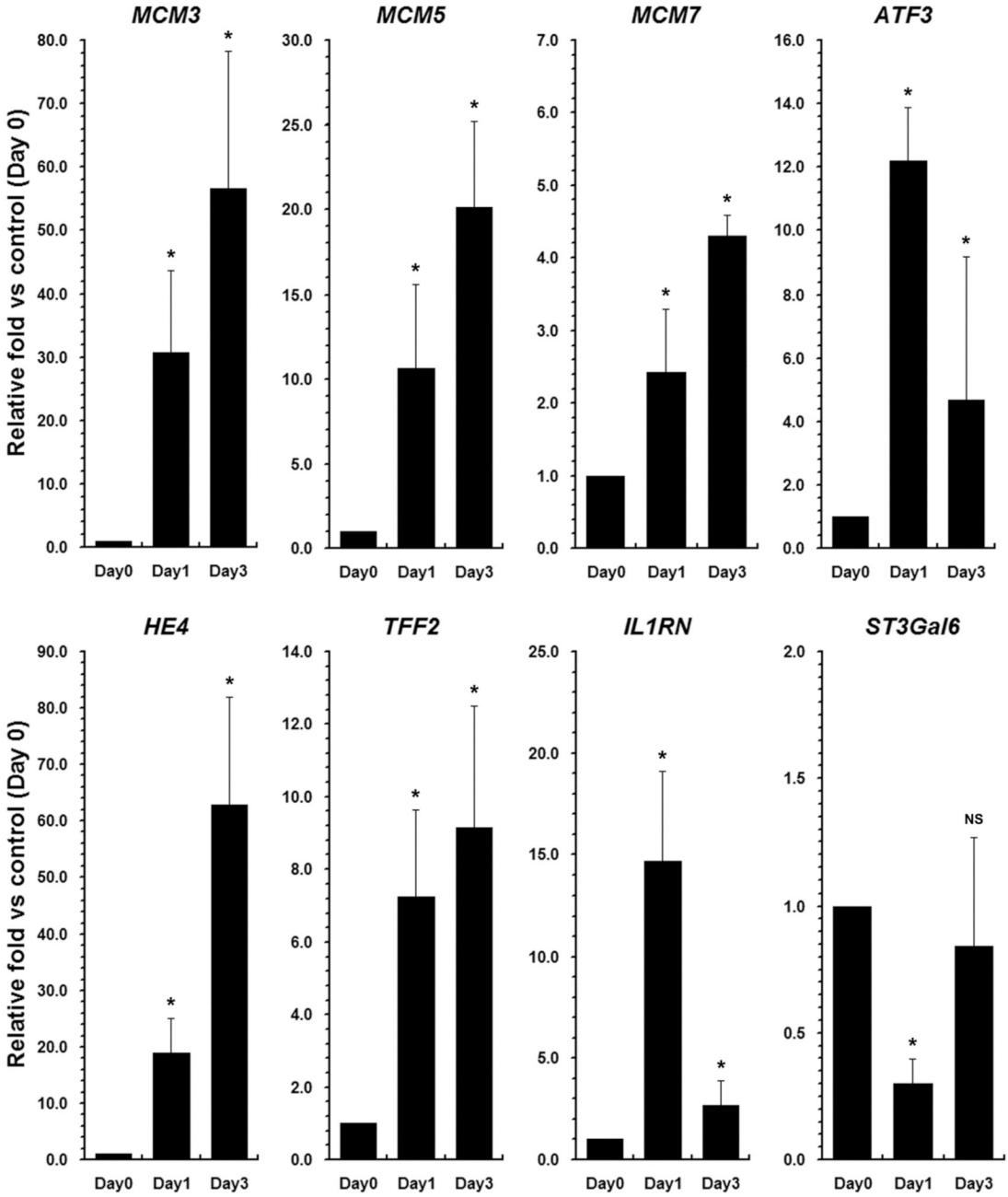

Figure 2. Quantitative PCR analysis of transcripts during the emergence of SPEM

Expression of selected up-regulated or down-regulated transcripts in microdissected lineages was examined using quantitative PCR to validate the results of the gene microarray studies. Results are represented as fold change in expression compared with levels in untreated chief cells (n=3, +/− standard error of the mean, SE). (* $p<0.05$ by Mann-Whitney *U*; NS, not significant)

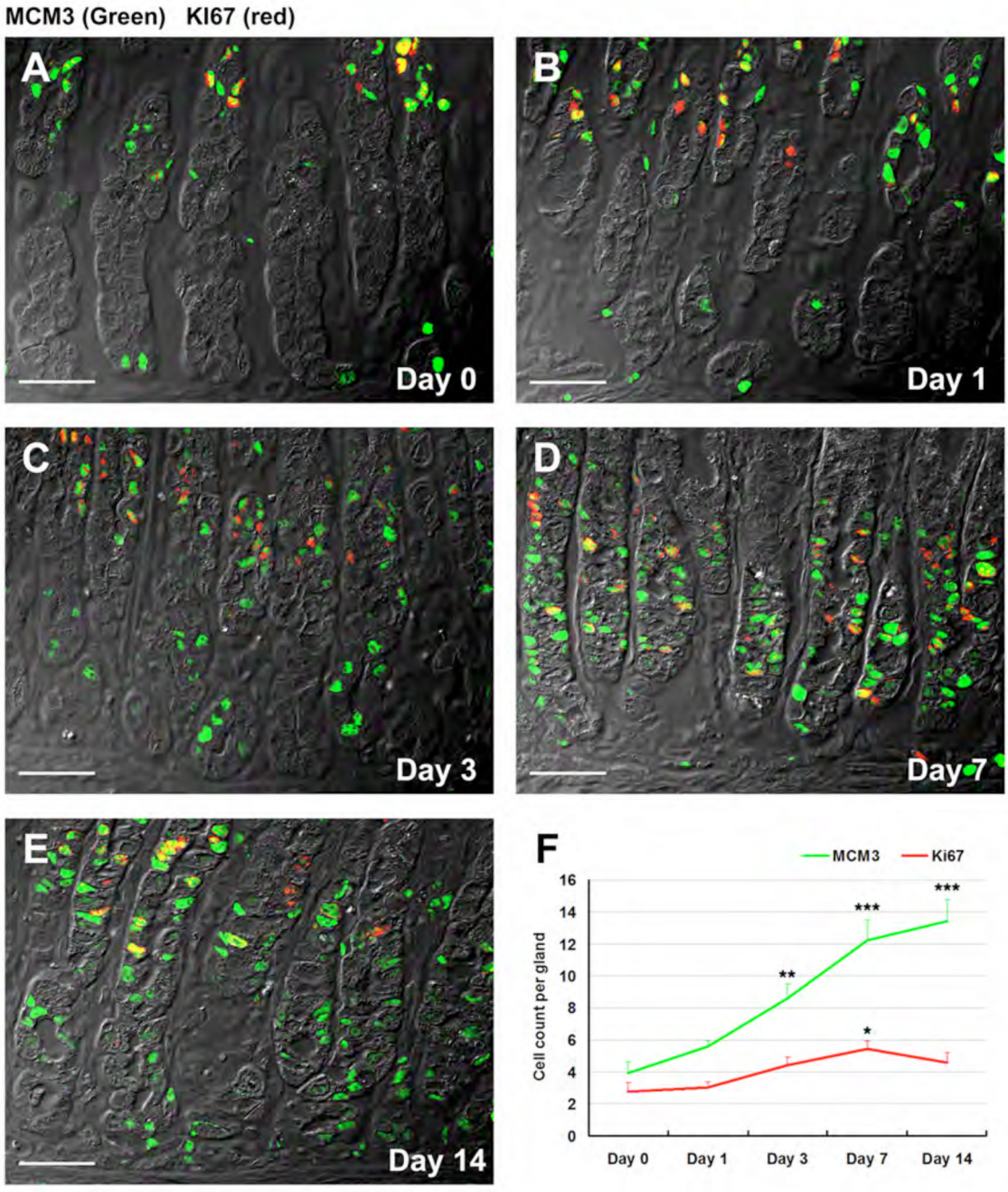

Figure 3. MCM3 expression during acute oxyntic atrophy

Sections from an untreated mouse **(A)** or mice treated with DMP-777 for 1 **(B)**, 3 **(C)**, 7 **(D)** or 14 **(E)** days were dual stained with antibodies against MCM3 (green) and antibodies against Ki67 (red). With increasing amounts of treatment DMP-777, we observed an increase in MCM3 staining in cells at the bases of glands (Scale bar: 40 μm). **(F)** Quantification of MCM3 and Ki-67 staining showed a significant increase in MCM3 staining at days 3–14 of treatment (green line, ** $p<0.01$; *** $p<0.001$). Ki-67 staining showed a smaller increase, which was only significant at 7 days of treatment (* $p<0.05$).

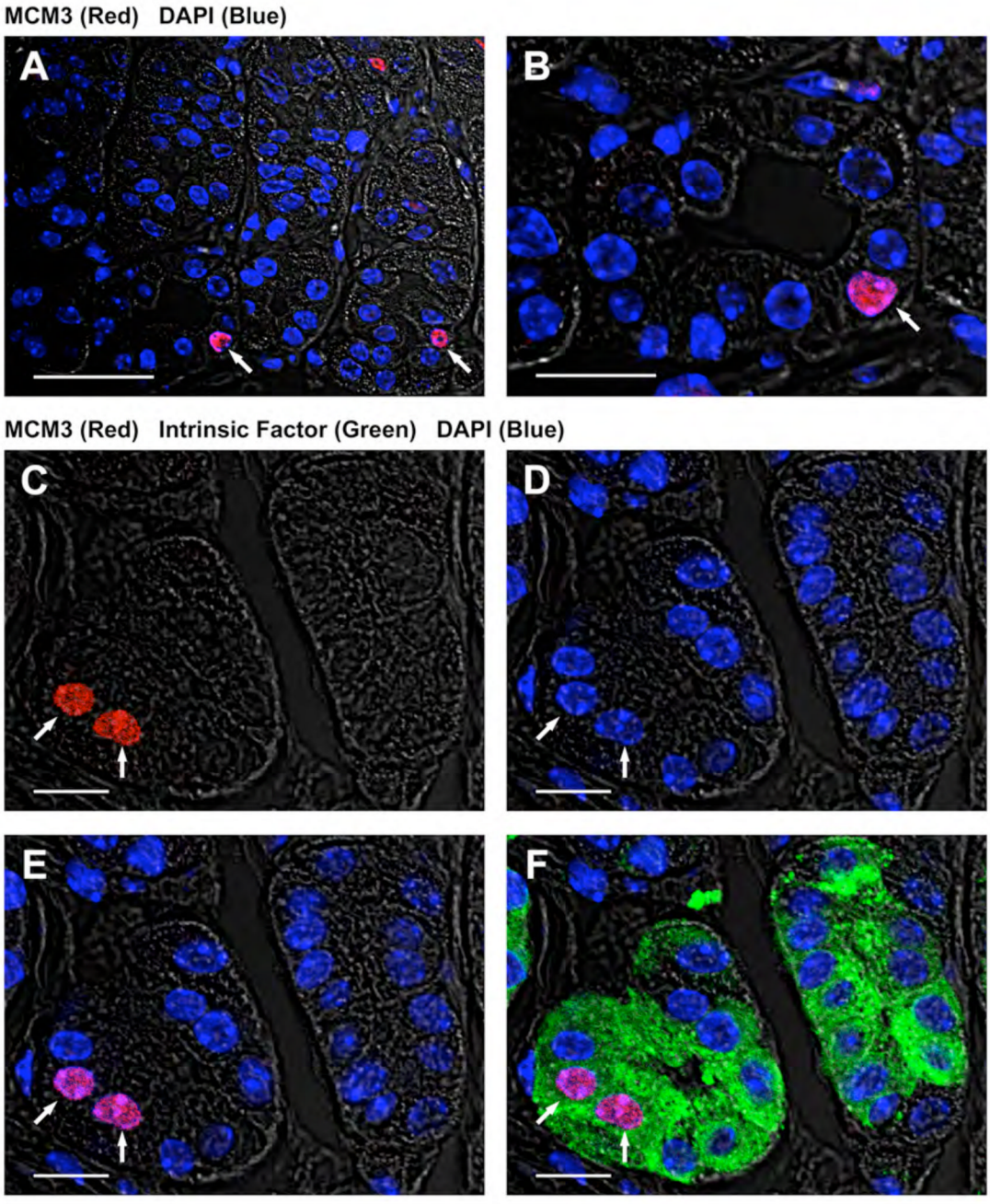

Figure 4. MCM3 positive cells at the bases of fundic glands in untreated mice are chief cells

Section from an untreated mouse stained with rabbit antibody against MCM3 (red), goat antibody against Intrinsic factor (green) and DAPI (blue). **(A–B)** Nuclear MCM3 expression observed in cells at the bases of fundic glands (Scale bar: **A**, 40 μm; **B**, 20 μm). **(C–F)** MCM3 positive cells at the bases of fundic glands were also stained for Intrinsic factor, indicating their identification as chief cells. **(C)** MCM3 positive cells (arrows) in the bottom of the fundic gland, **(D)** DAPI staining, **(E)** dual overlay image with MCM3 and DAPI, **(F)** triple overlay image with MCM3, Intrinsic Factor and DAPI. (Scale bar: **C–F**, 10 μm).

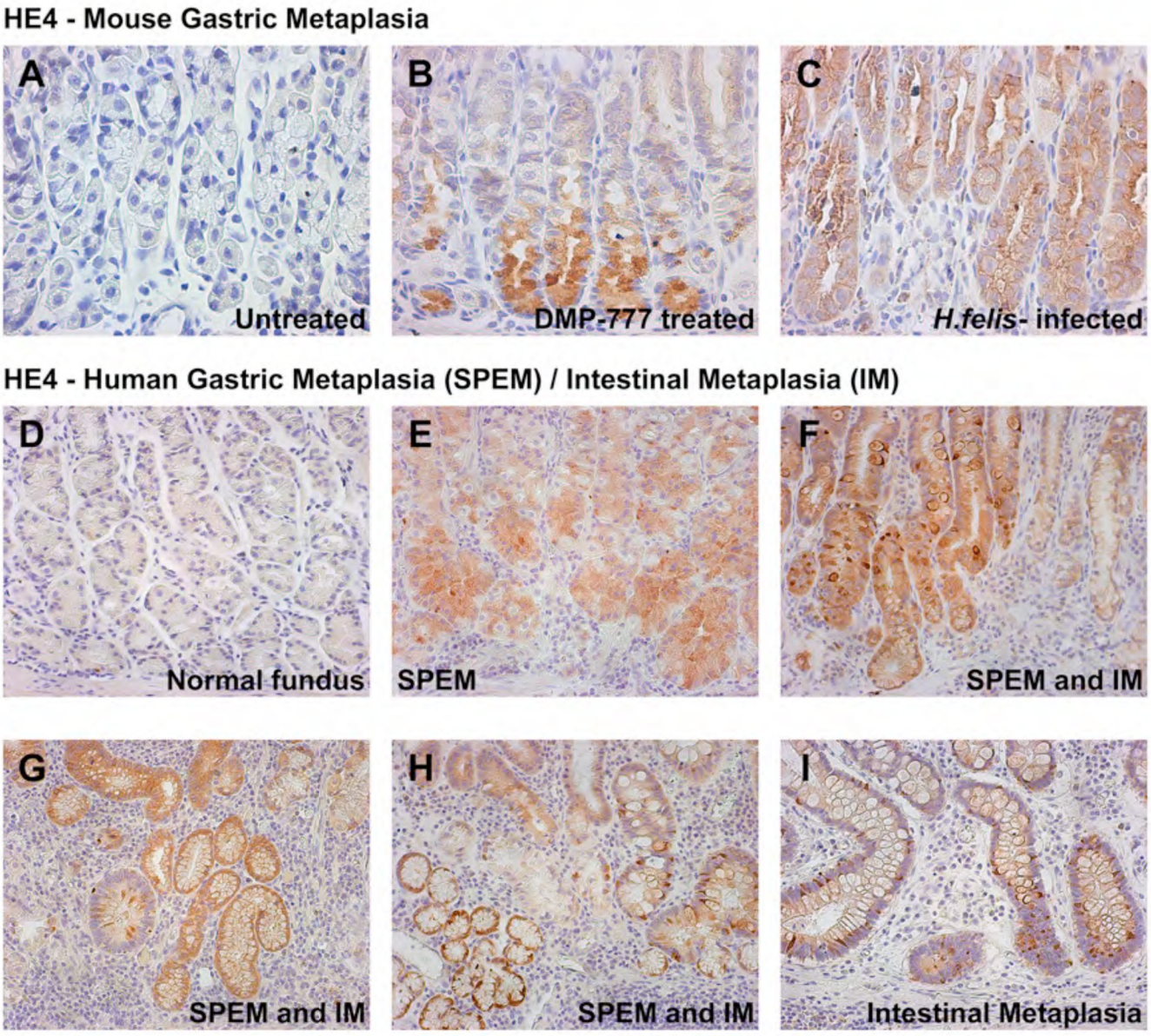

Figure 5. Up-regulation of HE4 in both SPEM and goblet cell intestinal metaplasia

We examined HE4 expression in gastric metaplasias from mice (**A–C**) and humans (**D–I**). **(A)** Little immunoreactivity for HE4 was detectable in the normal gastric mucosa of untreated gastrin-deficient mice. **(B)** Prominent staining for HE4 in SPEM in a gastrin deficient mouse treated with DMP-777. **(C)** Strong staining for HE4 was observed in SPEM in the mucosa of a C57BL/6 mouse infected with *Helicobacter felis* for 9 months. **(D)** No staining for HE4 was observed in the normal human gastric fundic mucosa. **(E)** SPEM from a human patient stained strongly with HE4. **(F)** SPEM and goblet cell intestinal metaplasia both stained for HE4 in a region of metaplastic transition. **(G, H)** In sections containing both SPEM and intestinal metaplasia, HE4 immunoreactivity was present in both metaplasias. **(I)** Intestinal metaplasia showing strong positivity for HE4.

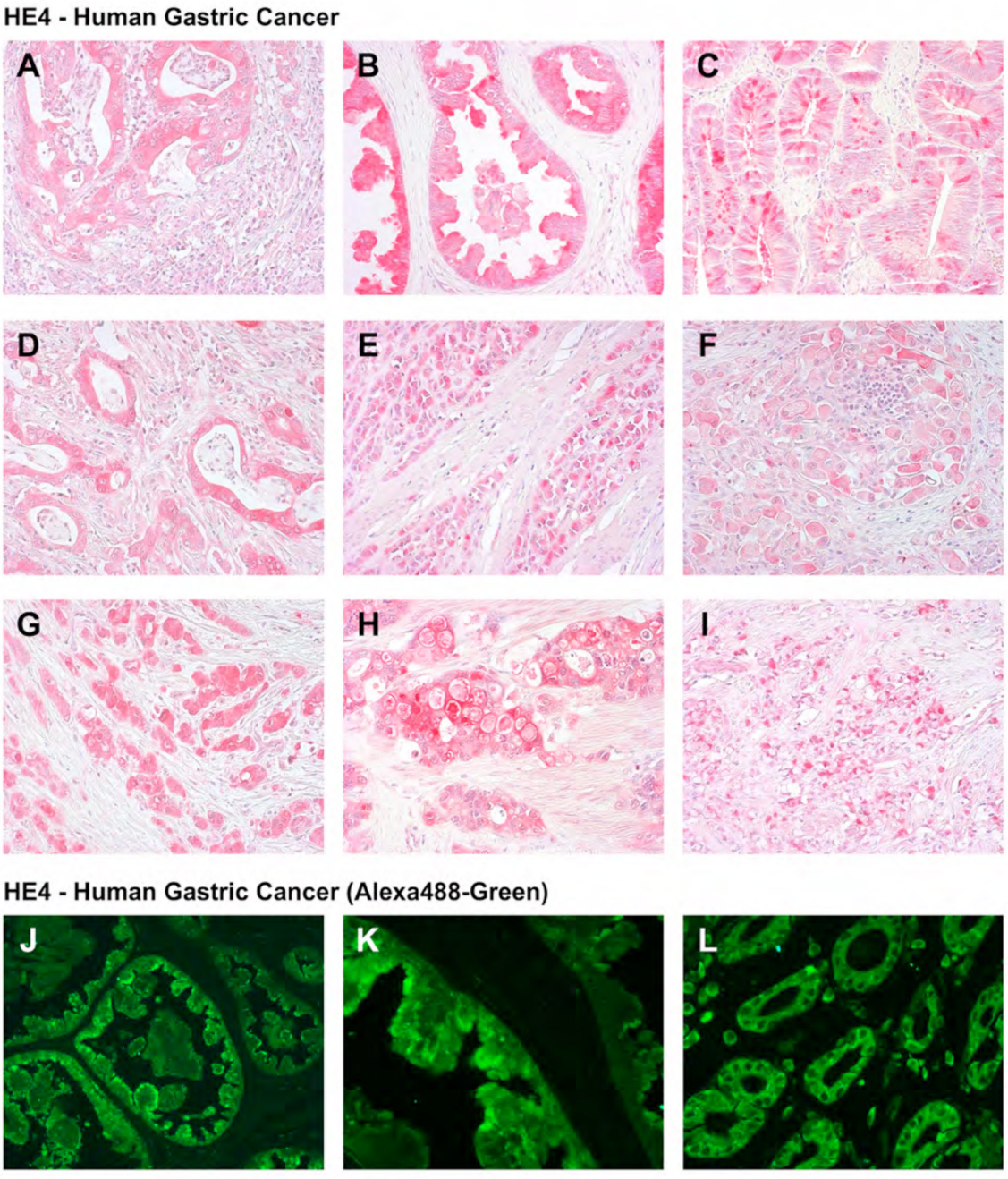

Figure 6. Immunostaining for HE4 in human gastric adenocarcinoma

HE4 antibodies were used to stain sections of gastric adenocarcinomas with immunohistochemical detection with alkaline phosphatase conjugated secondary antibody and Vector Red chromogen **(A–I). (A–D)** Well to moderately differentiated gastric cancers. Note the prominent expression of HE4 in intestinal type gastric adenocarcinoma. **(E–G)** Poorly-differentiated gastric cancers. Although the majority of poorly differentiated or diffuse cancers did not show immunoreactivity, a minority of tumors did show positivity. **(H, I)** Signet ring-cell type gastric adenocarcinomas. The strongest HE4 positivity was observed in signet ring adenocarcinomas. The positivity for HE4 in gastric cancers was also confirmed with immunofluorescence staining using Alexa488-anti-rabbit secondary

antibodies (green) **(J–L)**, supporting the immunohistochemical staining results for HE4 in gastric cancers.

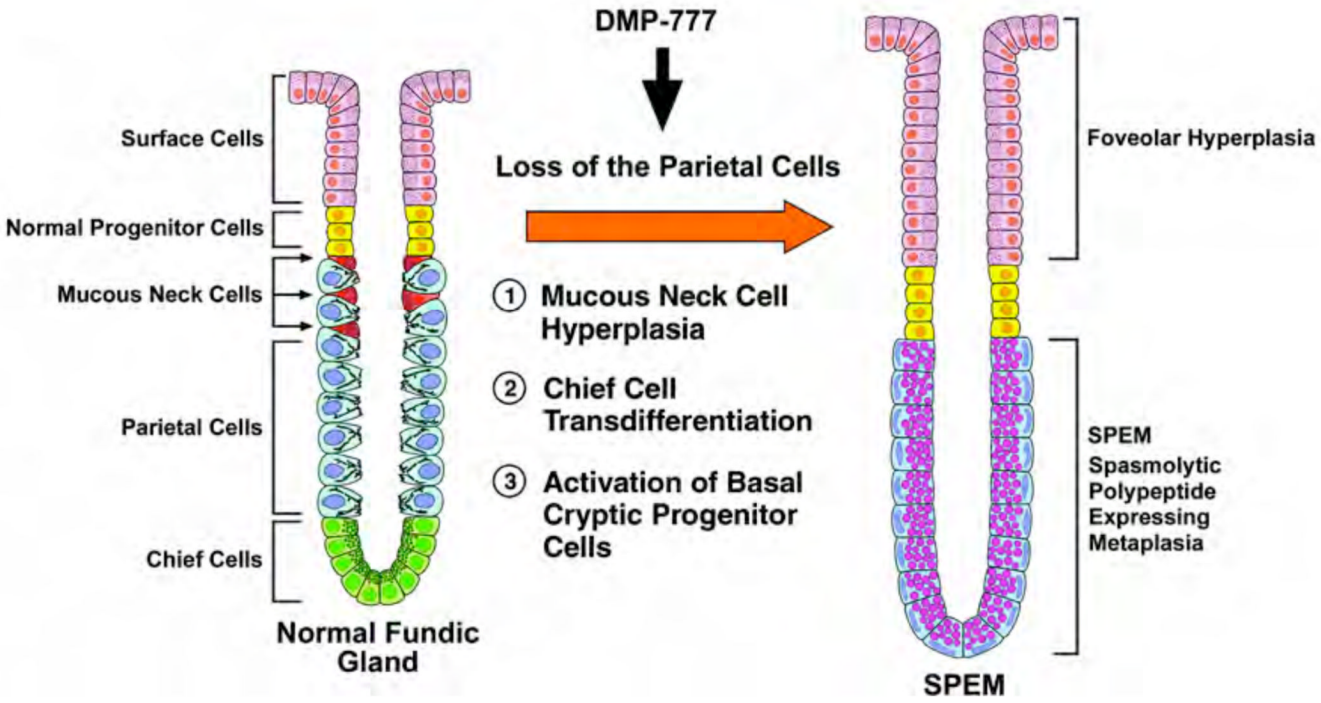

Figure 7. Hypothetical pathways for development of SPEM from gastric fundic glands

Three hypothetical pathways for the development of SPEM arising after acute parietal cell loss: 1, Mucous neck cell hyperplasia; 2, Transdifferentiation of chief cells; and 3, Activation of basal cryptic progenitor cells.

Table 1

Gene microarray analysis of the emergence of SPEM

(A) Probes in the top 50 up-regulated transcripts detecting messages associated with the cell cycle. **(B)** Putative secreted factors up-regulated in emerging SPEM. Fold increases in expression over control are indicated. A full listing of all transcripts significantly increased greater than 2-fold is shown in Supplemental Table 2.

A. Up-regulated Transcripts Associated with Cell Cycle			B. Up-regulated transcripts for soluble regulators		
Gene Symbo l	**1 DAY DMP-777 vs CONTRO L**	**3 DAYS DMP-777 vs CONTRO L**	**Gene Symbol**	**1 DAY DMP-777 vs CONROL**	**3 DAYS DMP-777 vs CONTROL**
Atf3	311.4	10.1	Lgals3	46.8	153.3
Uhrf1	35.3	8.8	Il1rn	25.4	18.5
Cenph	25.7	10.7	Trip13	10.3	8.6
Mcm6	25.1	36.4	Fignl1	10.2	6.6
Ris2*	21.5	41.3	Crip1	9.5	42.6
Mcm5 *	18.1	36.2	Wfdc2	8.9	67.5
Cdca5	17.3	36.1	Exosc8	6.2	6.7
Mcm5 *	13.9	18.2	WDNM1	5.2	345.9
Rad51	13.5	10.5	Ereg	3.6	28.9
Rad51ap1*	12.9	6.1			
Mcm10 *	12.2	31.3			
Cdc2a	11.7	7.0			
Tk1	10.1	11.5			
Clspn	9.5	8.5			
Lig1	9.3	9.6			
Cdca1	9.2	8.1			
Sssca1	8.9	12.3			
Dcc1	8.8	10.0			
Rad51ap1*	8.7	7.4			
Gadd45b	8.6	5.0			
Rfc4	8.5	8.4			
Rrm1	8.4	8.4			
Rfc3	8.1	6.1			

Gastroenterology. Author manuscript; available in PMC 2010 April 21.

A. Up-regulated Transcripts Associated with Cell Cycle			B. Up-regulated transcripts for soluble regulators		
Gene Symbo l	**1 DAY DMP-777 vs CONTRO L**	**3 DAYS DMP-777 vs CONTRO L**	**Gene Symbol**	**1 DAY DMP-777 vs CONROL**	**3 DAYS DMP-777 vs CONTROL**
Pole	7.5	11.3			
Ncapg	7.5	3.2			
Prc1	7.5	6.9			
Top2a	7.3	6.4			
Cdca8	7.3	8.7			
Ris2*	7.3	10.3			
Prc1	7.0	7.4			
Mcm10 *	6.7	10.1			
Rad54b	6.7	6.6			

* Indicates transcripts with multiple positive probes from the Affymetrix gene microarray. Results are expressed as fold increase in expression in samples from mice treated for either 1 or 3 days with DMP-777 compared to untreated controls.